Unveiling Charge Dynamics in Molecular Field-Coupled Nanocomputing

Roberto Listo*†¶, Federico Ravera*, Giuliana Beretta*, Yuri Ardesi*,
Gianluca Piccinini* and Mariagrazia Graziano‡
*Department of Electronics and Telecommunications, Politecnico di Torino, Torino 10129, Italy
†Department of Electrical, Computer and Biomedical Engineering, University of Pavia, Pavia 27100, Italy
‡Department of Applied Science and Technology, Politecnico di Torino, Torino 10129, Italy
¶Corresponding author e-mail: roberto.listo@polito.it

***Abstract*—Molecular Field-Coupled Nanocomputing (molFCN) emerges as a promising technology for addressing the challenges posed by CMOS scaling. In molFCN, the charge distribution of molecules encodes binary information. Properly arranging molecules in specific layouts produces wires and logic gates in which the information propagates by electrostatic intermolecular interaction with nearby molecules. Prior research offered promising insights into the static properties of information propagation within molFCN circuits, providing a theoretical description of the mechanism. However, the promising frequency-switching capabilities of molFCN still need to be validated. The frequency study of molecules is essential for ensuring the overall reliability of future molFCN devices. Consequently, this paper introduces a new methodology combining Density Functional Theory (DFT) and Real-Time Time-Dependent Density Functional Theory (RT-TDDFT) simulations for determining the maximum switching frequency of molFCN candidate molecules. We validate the methodology using the oxidized 1,4-diallyl butane molecule. Our findings demonstrate the possibility of achieving hundreds of gigahertz-level switching frequencies for the 1,4-diallyl butane. Moreover, the results report the nonlinear molecule behavior when subjected to electric field excitations above its charge-switching frequency limits. Overall, this work presents advances in addressing the time-domain modeling of molFCN candidate molecules, opening pathways for improving existing models for molFCN circuits.**

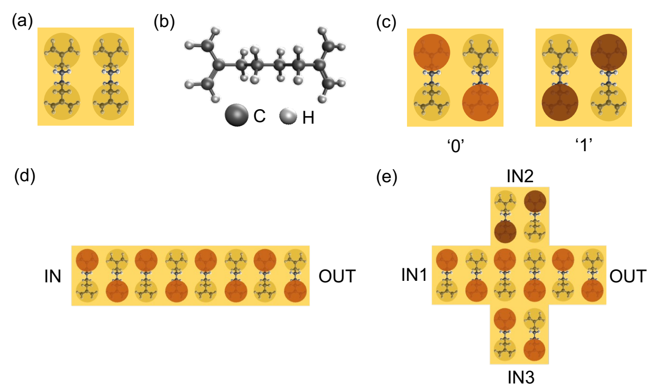

Fig. 1. An overview of the basics of molFCN technology. (a) Fundamental molFCN cell with four available aggregation centers for charge localization. (b) Structural view of the 1,4-diallyl butane molecule, exploited for the information encoding in the molFCN unit cell. (c) Possible logic states encoding through antipodal charge organization because of the minimization of the intermolecular electrostatic repulsion in the basic cell. (d) A molFCN wire comprising four aligned unit cells with '0' logic information propagated from the input to the output. (e) An example of molFCN majority voter circuit with the prevalence of the inputs assuming a '0' logic value, thus forcing a '0' to the output.

I. INTRODUCTION & BACKGROUND

Molecular Field-Coupled Nanocomputing (molFCN) is an emerging Beyond-CMOS computing technology that addresses the scaling challenges posed by CMOS [1]. The molFCN implements the Quantum-dot Cellular Automata (QCA) paradigm by exploiting charge localization within molecule charge aggregation regions to encode binary information [2]. Fig.1 (a) illustrates a schematic of the molFCN unit cell implemented with two 1,4-diallyl butane molecules. Fig.1 (b) shows the chemical structure of the 1,4-diallyl butane, which has been proposed as a molFCN candidate molecule in [2]. The charge within a couple of molecules antipodally distributes to reach the two possible electrostatically stable configurations associated with the logic information, as Fig.1 (c) reports. By adequately placing molFCN cells in ordered patterns, it is possible to obtain molFCN circuits in which the information propagates by electrostatic interactions between the coupled molecules [3]–[5]. Fig.1 (d) shows molFCN wire composed of four cells, whereas Fig.1 (e) reports the Majority Voter (MV) layout. The MV selects the most frequent input configuration and enables the implementation of AND and OR functions by fixing one of the inputs to '0' and '1', respectively. In general, the molFCN technology presents numerous advantages as low power consumption due to the absence of current flow during information propagation, the possibility to create high-density devices thanks to the nanometric molecular size, and the ability to work at ambient temperature [6]–[9]. Extensive research is conducted on molFCN circuits at both the single-molecule [10]–[13] and circuit design levels, primarily focusing on time-independent characterizations [14]–[17]. In particular, we have proposed the Molecular Simulator Quantum-dot Cellular Automata Torino (MoSQuiTo) methodology, which implements a three-step approach to analyze molFCN circuit starting from the single-molecule electrostatic characterization [5]. In MoSQuiTo, results from *ab initio* investigations permit modeling the molFCN candidate molecules as electronic devices. Then, the produced characteristics are used to evaluate information propagation in molFCN circuits with the Self-Consistent ElectRostatic Potential Algorithm (SCERPA), which iteratively solves the electrostatic interactions within molecules in the layout [16], [18], [19]. Therefore, the MoSQuiTO methodology allows molFCN circuit design considering molecules electrostatics and also permitting the introduction of non-idealities in the circuit layout, overall overcoming current idealizations in molFCN designs [20]–[23]. Despite the numerous advantages of molFCN and its theoretical capability to operate in the THz range [9], [24], time-dependent circuit-level studies that integrate molecular physics still need to be introduced. Indeed, studying frequency limitations in molFCN is crucial for a technologically comprehensive assessment such as power efficiency evaluation and operational temperature regimes. Moreover, the single-molecule frequency study would improve the MoSQuiTO methodology by permitting assessing the time-dependent information propagation analysis. Therefore, this paper studies the time behavior of the 1,4-diallyl butane, which has been much studied in the molFCN context as a candidate molecule. Specifically, the manuscript presents a methodology for identifying the maximum switching frequency of molFCN candidate molecules, focusing on studying the charge delocalization within the charge aggregation regions. Precisely, the study is composed of two key phases. Initially, a static characterization examines the molecule in isolation and when subjected to static electric fields. The static characterization is conducted through *ab initio* simulations and demonstrates the charge-switching capabilities of the candidate molecule. Then, a frequency-dependent analysis is conducted, employing time-varying external electric fields and Real-Time Time-Dependent Density Functional Theory (RT-TDDFT). The results demonstrate the suitability of the proposed methodology for analyzing the 1,4-diallyl butane. Specifically, two time-varying regime simulations were conducted at 640 GHz and 64 THz. Interestingly, the results at 64 THz show non-linearities in charge switching, resulting in spurious variations of the logic value encoded by the molecule.

Overall, the results suggest the correct behavior of the 1,4-diallyl butane molecule when stimulated by electric fields varying in the thousands of GHz regime. The methodology adopted in this work set the ground for future studies in the molFCN time-dependent characteristics, specifically regarding molecule modeling for future increasingly comprehensive simulation of molFCN circuits.

II. ASSESSMENT OF MOLFCN CHARGE DYNAMICS

This section presents the methodology employed for the frequency analysis of molFCN candidate molecules. We delineate two analysis phases, focusing on static and dynamic studies. The molecule static characterization is conducted with DFT simulations, whereas RT-TDDFT calculations are used for exploring the time-dependent properties. We focus on the 1,4-diallyl butane molecule to analyze the intramolecular charge transfer. Specifically, we examine the dipole moment as the most suitable parameter for studying charge localization. The results have been obtained with NWChem, Q-Chem, and IQmol [25]–[28].

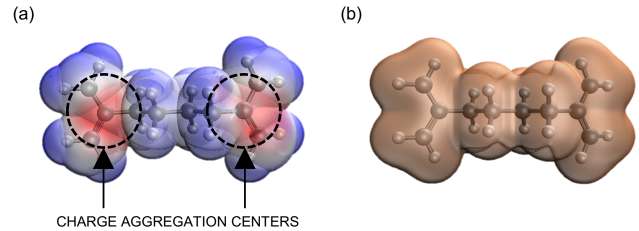

Fig. 2. Characterization of the 1,4-diallyl butane ground state relaxed geometry. The results are obtained withIQmol with STO-6G BS, CAM-B3LYP XC, and D3 DC. (a) Graphical visualization of the electrostatic potential. (b) Graphical visualization of the total charge density.

A. Static characterization of molFCN molecules

Molecule static characterization provides the essential tools and awareness to interpret dynamic regime results. Furthermore, it defines the molecule suitability for molFCN applications. The study accurately describes the state of the molecule both at equilibrium and when subjected to constant electric field excitation, providing the ground for successive time-dependent analyses. The static analysis is conducted using a three-step approach: geometry optimization (S1), ground state analysis (S2), and constant external excitation analysis (S3). S1 consists of determining the ground state geometry of the molecule. This phase is of fundamental importance since the precision of the following simulation results is strongly dependent on the accuracy of the geometry optimization. Therefore, it is essential to appropriately choose the Basis Set (BS), the Exchange Correlation Functional (XC), and the Dispersion Correction (DC) in such a way as to guarantee precise molecule description. In the case of the geometry optimization of the 1,4-diallyl butane molecule, we used NWChem with Def2-TZVP as BS, CAM-B3LYP as XC, and D3 as DC [28]–[31]. In S2, taking the optimized geometry obtained in S1, we analyze the molecule electronic properties in the ground state. Specifically, we evaluate the dipole moment, the electrostatic potential, and the electron density distribution. The dipole moment and the electron density distribution measure the initial state of the charge distribution within the molecule, whereas the electrostatic potential gives more details on the charge aggregation sites and information encoding. The simulation results of S2 for the 1,4-diallyl butane molecule are executed using IQmol, employing STO-6G as BS, B3LYP as XC, and D3 as DC. Fig.2 (a) illustrates the electrostatic potential distribution of the oxidized 1,4-diallyl butane molecule, revealing its charge aggregation centers associated with the two allyl groups. Moreover, Fig.2 (b) displays the total charge distribution of the oxidized 1,4-diallyl butane molecule, which exhibits charge delocalization across the molecule. The dipole moment magnitude of 1,4-diallyl butane in its ground state equals 0.001 D, confirming the global charge delocalization. In S3, multiple

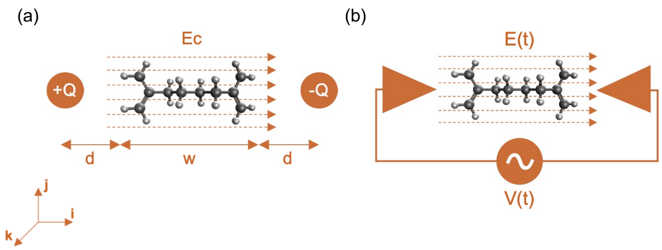

Fig. 3. A schematic view of the 1,4-diallyl butane molecule static and dynamic analysis simulation setup. (a) Two point charges are equidistantly positioned to generate a constant electric field Ec that excites the 1,4-diallyl butane molecule. (b) Conceptual simulation setup for exciting the 1,4-diallyl butane molecule with a time-varying external electric field E(t).

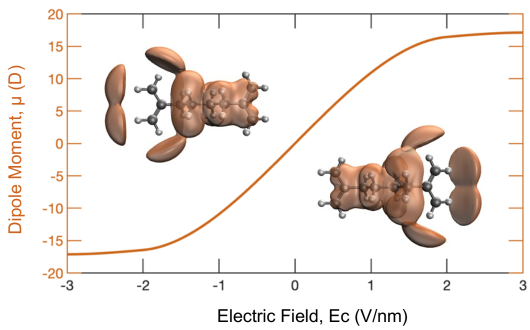

Fig. 4. transcharacteristic of the dipole moment versus electric field of the 1,4-diallyl butane molecule obtained trough DFT simulations performed with NWChem using Def2-TZVP as BS, CAM-B3LYP as XC, and D3 as DS.

DFT simulations are performed, starting from the molecule ground state and applying a set of constant external electric fields generated by two point charges positioned as depicted in Fig.3 (a). The distance between the molecule and point charges and the value of the point charges determines the electric field experienced by the molecule. Precisely, the electric field is evaluated as

$$Ec = |\mathbf{E}(Q,d)| = 2\,\frac{1}{4\pi\epsilon_0}\,\frac{|Q|}{(d+\frac{w}{2})^2} \tag{1}$$

where ϵ_0 is the vacuum permittivity, d denotes the distance between the charges and the molecule, and Q represents the value of the point charges. For each electric field intensity, the corresponding dipole moment of the molecule is calculated, and a transcharacteristic of the dipole moment versus the electric field is generated. Fig.4 depicts the transcharacteristic of the 1,4-diallyl butane for electric field intensities ranging from -3 $\mathrm{V/nm}$ to 3 $\mathrm{V/nm}$. Notably, a saturation region is observed for the external electric field below -1 $\mathrm{V/nm}$ and above 1 $\mathrm{V/nm}$. Fig.4 shows two significant images representing the charge localization in the saturation regions. Further increasing the electric field above the field saturation values leads to minimal dipole moment variation. The results are coherent with those obtained in [32]. The transcharacteristic proves the capability of the 1,4-diallyl butane molecule to localize the charge in two distinguished sites of the molecule, assessing its suitability for molFCN application. Moreover, it serves as a reference for understanding the impact of the time-varying exciting electric field on the dipole moment variation. Indeed, it provides the reference value of the dipole moment in the static regime corresponding to a specific electric field intensity. This value will be compared to the amplitude of the dipole moment corresponding to the same electric field intensity in the time-varying analysis. Such comparison enables estimating and quantifying possible dipole moment attenuations of the magnitude corresponding to the operating frequency under study. Overall, the results obtained from the static characterization serve as the foundation for the dynamic simulation results, providing a reference for verifying attenuation mechanisms arising in the time-varying regime in which the molecule is studied.

B. Dynamic characterization of molFCN molecules

In the proposed methodology, we approach the study of charge dynamics within the molecule. Specifically, we subject the molecule to time-varying electric fields to observe the resulting dipole moment variation, thus evaluating the molecular charge reactive response to external excitation. The ultimate goal in analyzing the dipole moment variation in response to time-varying electric fields is to find the operational limits of the molecule in terms of charge switching. Specifically, the frequency for which the charge movement in the molecule is delayed to the applied field stimulation should be sought, thus establishing an operating frequency limit for the molFCN candidate molecule. Fig.3 (b) depicts the conceptual simulation setup used to analyze the frequency behavior of the candidate molecule. The molecule is positioned between two ideal electrodes connected to a time-varying voltage source. Upon activation of the voltage source, the molecule experiences a time-varying electric field, represented by three components:

$$\mathbf{E}(t) = E_x(t)\hat{\mathbf{i}} + E_y(t)\hat{\mathbf{j}} + E_z(t)\hat{\mathbf{k}} \tag{2}$$

Each component reflects its contribution along the axis $\mathbf{i}$, $\mathbf{j}$, and $\mathbf{k}$, as Fig.3 shows. Given our focus on the molecule response to specific frequencies, we utilize the RT-TDDFT method to analyze the dipole moment variation over time when the molecule is subjected to a sinusoidal electric field. Consequently, the three components of the electric field are:

$$E_x(t) = A\sin(2\pi f t) \tag{3}$$

$$E_y(t) = E_z(t) = 0 \tag{4}$$

where A represents the electric field intensity, whereas f and (t) denote the frequency and time, respectively. This dipole moment time variation is obtained by solving the Time-Dependent Kohn–Sham (TD-KS) equation for the molFCN molecule:

$$i\hbar\frac{\partial}{\partial t}\psi_i(\mathbf{r},t) = \left[-\frac{\hbar^2}{2m}\nabla^2 + V_{\mathrm{KS}}(\mathbf{r},t)\right]\psi_i(\mathbf{r},t) \tag{5}$$

where $V_{\mathrm{KS}}(\mathbf{r},t) = V_{\mathrm{ext}}(\mathbf{r},t) + V_{\mathrm{H}}(\mathbf{r},t) + V_{\mathrm{xc}}[\rho](\mathbf{r},t)$. In this equation $\psi_i(\mathbf{r},t)$ represents the time-dependent Kohn-Sham orbitals, $V_{\mathrm{ext}}(\mathbf{r},t)$ is the external potential, $V_{\mathrm{H}}(\mathbf{r},t)$ is

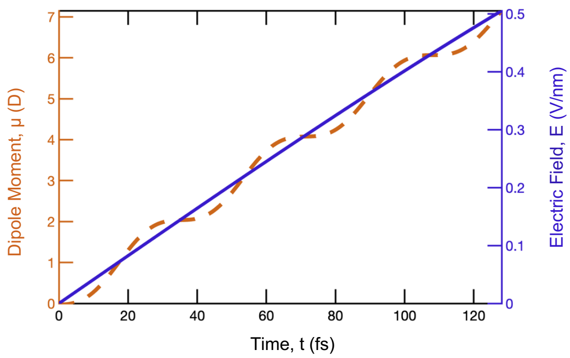

Fig. 5. The 1,4-diallyl butane dipole moment response to a time-varying sinusoidal electric field at 640 GHz and the exciting electric field. The dipole moment follows the electric field variation. Therefore, the molecule switches correctly at 640 GHz.

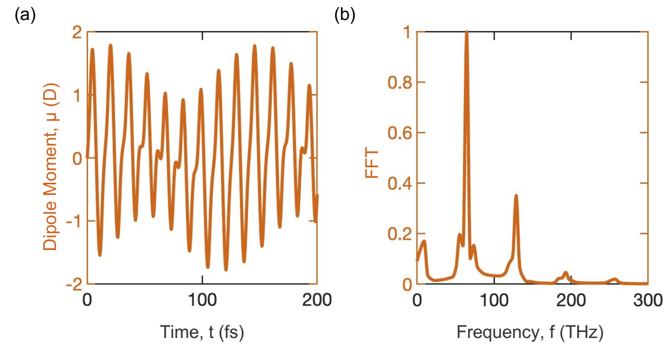

Fig. 6. The 1,4-diallyl butane dipole moment response to a time-varying sinusoidal electric field at 64 THz. (a) The dipole moment variation over time. (b) The single-sided FFT of the dipole moment. The dipole moment variation is strongly affected by nonlinear effects, causing the impossibility of localizing the charge in one of the two aggregation centers.

the Hartree potential, $V_{\rm xc}[\rho](\mathbf{r},t)$ is the exchange-correlation potential, ρ is the electron density, m is the electron mass, and $\hbar$ is the reduced Planck constant [31]. RT-TDDFT simulations require careful parameter selection to ensure convergence and reliable outcomes. First, it is essential to choose the BS, XC, and DC to describe electronic delocalization in the molecule accurately. For the study of 1,4-diallyl butane, we employed def2-TZVP as BS; it offers a good balance between computational efficiency and accuracy and provides a high level of precision in describing electron correlation and molecular orbitals, CAM-B3LYP as XC for its hybrid nature, by combining both long-range corrected and conventional hybrid functional approaches it is particularly effective in capturing charge transfer excitations and provides an accurate description of electronic transitions, and D3 as DS for precisely accounting van der Waals interactions. Subsequently, the electric field intensity is determined to balance charge delocalization effectiveness and simulation convergence, with a value of 1 V/nm chosen for our study. Moreover, the time step for temporal analysis must be selected carefully to ensure result reliability. As suggested in [28], a low time step enhances simulation convergence and result accuracy. For our study of 1,4-diallyl butane, a time step of 0.02419 fs fulfills these requirements.

To validate the methodology and its efficacy in studying the 1,4-diallyl butane molecule charge-switching capability, we selected two distinct frequencies: 640 GHz and 64 THz. Analyzing these two frequencies permits evaluating both operating states of the charge-switching mechanism. Specifically, a proper operation in which the charge moves at the same frequency as the electric field and one at a high frequency, which does not allow the charge to move correctly due to nonlinear phenomena. Fig.5 reports the dipole moment variation in a 130 fs span and the associated external electric field excitation at 640 GHz. The electric field reaches a maximum value of 0.5 V/nm during the time window under analysis. As Fig.5 shows, the molecule dipole moment follows the variations induced by the electric field. Remarkably, the dipole moment values observed over

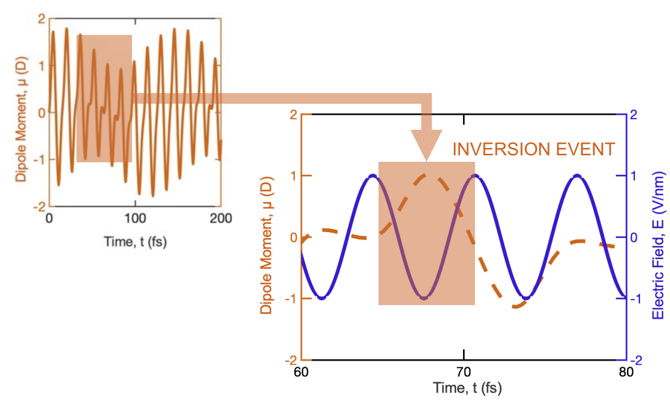

Fig. 7. A zoom on the inversion mechanism that brings to an error in the information encoding associated with a time-varying sinusoidal electric field at 64 THz. Despite the electric field being positive in the highlighted region, the dipole moment is negative, suggesting that the charge localizes in the opposite direction to what is expected based on the direction of the electric field.

time are coherent with those reported in the static regime characterization. Furthermore, focusing on the 0.5 V/nm excitation highlighted in the static transcharacteristic in Fig.2, the associated dipole moment is of 7 D. The same dipole moment value is reported by Fig.5 when the external electric field reaches 0.5 V/nm. The coherence between temporal and static regime dipole moment values validates the results obtained in the static analysis. Moreover, it demonstrates the possibility of operating the 1,4-diallyl butane at frequencies up to 640 GHz, given the proper dynamic charge arrangement showcased by the molecule. Contrarily, when the electric field frequency increases over a certain threshold, the charge within the molecule does not rearrange following the induced variations. In this condition, nonlinear effects, possibly due to the intramolecular charge reorganization, arise, leading to the impossibility of adequately localizing charge within the molecule aggregation centers. Fig.6 (a) reports the dipole moment variation in a 200 fs span on the 1,4-diallyl butane molecule when subjected to a 64 THz sinusoidal electric field. In this case, the dipole moment variation reports nonlinearities, highlighted by spurious variations in the dipole moment values. Moreover, the μ values oscillate between -1 D and 1 D, lower than expected for the 1 V/nm electric field amplitude, thus indicating the absence of concrete charge localization within the molecule. The FFT associated with the dipole moment in Fig.6 (b) confirms the presence of frequency components differing from that of the external field influencing the molecule. The nonlinear effects affect the charge localization within the charge aggregation centers and may cause errors in the information. Fig.7 further highlights the presence of nonlinearities. Specifically, the dipole moment exhibits counter-phase behavior while failing to follow the electric field trend. From a molFCN system point of view, this effect results in the encoding of logic values opposite to those one would like to impose in the molecule at a given frequency, compromising the stability and correctness of the resulting propagating system.

Overall, the proposed RT-TDDFT simulations offers a novel approach for analyzing molFCN candidate molecules in the frequency domain, facilitating the switching mechanism assessment. Specifically, we demonstrated the correct charge-switching of the 1,4-diallyl butane molecule up to 640 GHz, whereas nonlinearities arise in the 64 THz domain. The methodology can be used to determine the maximum operating frequency and be the basis for dipole moment time-dependent models of molFCN candidate molecules. The analysis of the molecule models will lay a robust foundation for future molFCN time-domain circuit modeling.

III. CONCLUSION

This paper presented a methodology for investigating the frequency constraints of charge localization within molFCN molecules. We delineate two study phases corresponding to static and dynamic analyses. The static characterization, conducted via DFT simulations, assesses the suitability of the molecule under test for molFCN applications and provides a foundation for interpreting results from the dynamic regime obtained through RT-TDDFT simulations. We adopt the methodology using the oxidized 1,4-diallyl butane molecule, demonstrating its capability to successfully switch the charge in its charge aggregation centers in response to external electric field excitation at frequencies as high as 640 GHz. Furthermore, this work presented the nonlinear effects and errors in the charge localization arising from a too-high-frequency electric field excitation. Specifically, the nonlinear effects have been observed in the case of a 64 THz stimulating external electric field, and we demonstrated them to cause spurious charge distribution inversions. Overall, our methodology lays a robust groundwork for future modeling of the frequency response of individual molFCN molecules. It enables the identification of the maximum operating frequency of the single molFCN molecule and permits to derivation of an equivalent electrical model of the molecule in the frequency domain. The equivalent electrical model will form the basis for the time domain modeling of entire molFCN circuits, thereby facilitating the determination of their maximum operating frequency. Understanding the maximum operating frequency opens pathways to analyzing the overall power consumption, energy needs, heat dissipation, and dynamic investigations at the molFCN device level.

REFERENCES

[1] (2023) International roadmap for devices and systems. IEEE. [Online]. Available: https://irds.ieee.org/editions/2023

[2] C. S. Lent, B. Isaksen, and M. Lieberman, "Molecular quantum-dot cellular automata," *Journal of the American Chemical Society*, vol. 125, no. 1, pp. 1056–1063, 2003.

[3] C. Lent and B. Isaksen, "Clocked molecular quantum-dot cellular automata," *IEEE Transactions on Electron Devices*, vol. 50, no. 9, pp. 1890–1896, 2003.

[4] S. C. Chetti and O. Yatgal, "Qca: A survey and design of logic circuits," *Global Transitions Proceedings*, vol. 3, no. 1, pp. 142–148, 2022.

[5] A. Pulimeno, M. Graziano, A. Antidormi, R. Wang, A. Zahir, and G. Piccinini, "Understanding a bisferrocene molecular qca wire," in *Proceedings of the International Workshop on Molecular and Nanoscale Communication*. Berlin, Heidelberg: Springer Berlin Heidelberg, 2014, pp. 307–338.

[6] E. P. Blair, E. Yost, and C. S. Lent, "Power dissipation in clocking wires for clocked molecular quantum-dot cellular automata," *Journal of Computational Electronics*, vol. 9, pp. 49–55, 2010.

[7] J. Timler and C. S. Lent, "Power gain and dissipation in quantum-dot cellular automata," *journal of applied physics*, vol. 91, no. 2, pp. 823–831, 2002.

[8] Y. Ardesi, A. Gaeta, G. Beretta, G. Piccinini, and M. Graziano, "Ab initio molecular dynamics simulations of field-coupled nanocomputing molecules," *Journal of Integrated Circuits and Systems*, vol. 16, no. 1, pp. 1–8, 2021.

[9] Y. Wang and M. Lieberman, "Thermodynamic behavior of molecular-scale quantum-dot cellular automata (qca) wires and logic devices," *IEEE Transactions on Nanotechnology*, vol. 3, no. 3, pp. 368–376, 2004.

[10] Y. Lu and C. S. Lent, "Theoretical study of molecular quantum-dot cellular automata," *Journal of Computational Electronics*, vol. 4, pp. 115–118, 2005.

[11] B. Tsukerblat, A. Palii, and S. Aldoshin, "Molecule based materials for quantum cellular automata: A short overview and challenging problems," *Israel Journal of Chemistry*, vol. 60, no. 5-6, pp. 527–543, 2020.

[12] V. Arima *et al.*, "Toward quantum-dot cellular automata units: thiolated-carbazole linked bisferrocenes," *Nanoscale*, vol. 4, no. 3, pp. 813–823, 2012.

[13] N. Liza, D. Murphey, P. Cong, D. W. Beggs, Y. Lu, and E. P. Blair, "Asymmetric, mixed-valence molecules for spectroscopic readout of quantum-dot cellular automata," *Nanotechnology*, vol. 33, no. 11, p. 115201, 2021.

[14] C. S. Lent, M. Liu, and Y. Lu, "Bennett clocking of quantum-dot cellular automata and the limits to binary logic scaling," *Nanotechnology*, vol. 17, no. 16, p. 4240, 2006.

[15] G. Beretta, Y. Ardesi, G. Piccinini, and M. Graziano, "Robustness of the in-plane data crossing for molecular field-coupled nanocomputing," in *2023 IEEE 23rd International Conference on Nanotechnology (NANO)*. IEEE, 2023, pp. 732–736.

[16] Y. Ardesi, U. Garlando, F. Riente, G. Beretta, G. Piccinini, and M. Graziano, "Taming molecular field-coupling for nanocomputing design," *ACM Journal on Emerging Technologies in Computing Systems*, vol. 19, no. 1, pp. 1–24, 2022.

[17] Y. Ardesi, L. Gnoli, M. Graziano, and G. Piccinini, "Bistable propagation of monostable molecules in molecular field-coupled nanocomputing," in *2019 15th Conference on Ph. D Research in Microelectronics and Electronics (PRIME)*. IEEE, 2019, pp. 225–228.

[18] Y. Ardesi, R. Wang, G. Turvani, G. Piccinini, and M. Graziano, "Scerpa: A self-consistent algorithm for the evaluation of the information propagation in molecular field-coupled nanocomputing," *IEEE Transactions on Computer-Aided Design of Integrated Circuits and Systems*, vol. 39, no. 10, pp. 2749–2760, 2019.

[19] G. Beretta, Y. Ardesi, G. Piccinini, and M. Graziano, "Scerpa v4.0.1," Dec. 2022. [Online]. Available: https://github.com/vlsinanocomputing/scerpa

[20] M. Graziano, R. Wang, M. R. Roch, Y. Ardesi, F. Riente, and G. Piccinini, “Characterisation of a bis-ferrocene molecular qca wire on a non-ideal gold surface,” *Micro & Nano Letters*, vol. 14, no. 1, pp. 22–27, 2019.

[21] Y. Ardesi, G. Beretta, M. Vacca, G. Piccinini, and M. Graziano, “Impact of molecular electrostatics on field-coupled nanocomputing and quantum-dot cellular automata circuits,” *Electronics*, vol. 11, no. 2, p. 276, 2022.

[22] F. Ravera, G. Beretta, Y. Ardesi, M. Krzywiecki, M. Graziano, and G. Piccinini, “A roadmap for molecular field-coupled nanocomputing actualization,” in *2023 IEEE Nanotechnology Materials and Devices Conference (NMDC)*. IEEE, 2023, pp. 212–213.

[23] K. Walus, T. J. Dysart, G. A. Jullien, and R. A. Budiman, “Qcadesigner: A rapid design and simulation tool for quantum-dot cellular automata,” *IEEE transactions on nanotechnology*, vol. 3, no. 1, pp. 26–31, 2004.

[24] Y. Lu, M. Liu, and C. Lent, “Molecular quantum-dot cellular automata: From molecular structure to circuit dynamics,” *Journal of applied physics*, vol. 102, no. 3, 2007.

[25] M. R. Provorse and C. M. Isborn, “Electron dynamics with real-time time-dependent density functional theory,” *International Journal of Quantum Chemistry*, vol. 116, no. 10, pp. 739–749, 2016.

[26] K. Lopata and N. Govind, “Modeling fast electron dynamics with real-time time-dependent density functional theory: Application to small molecules and chromophores,” *Journal of chemical theory and computation*, vol. 7, no. 5, pp. 1344–1355, 2011.

[27] Y. Shao *et al.*, “Advances in molecular quantum chemistry contained in the q-chem 4 program package,” *Molecular Physics*, vol. 113, no. 2, pp. 184–215, 2015.

[28] E. Apra *et al.*, “Nwchem: Past, present, and future,” *The Journal of chemical physics*, vol. 152, no. 18, 2020.

[29] T. Yanai, D. P. Tew, and N. C. Handy, “A new hybrid exchange–correlation functional using the coulomb-attenuating method (cam-b3lyp),” *Chemical physics letters*, vol. 393, no. 1-3, pp. 51–57, 2004.

[30] L. Goerigk, “A comprehensive overview of the dft-d3 london-dispersion correction,” *Non-covalent interactions in quantum chemistry and physics*, pp. 195–219, 2017.

[31] K. Burke, J. Werschnik, and E. Gross, “Time-dependent density functional theory: Past, present, and future,” *The Journal of chemical physics*, vol. 123, no. 6, 2005.

[32] Y. Ardesi, M. Graziano, and G. Piccinini, “A model for the evaluation of monostable molecule signal energy in molecular field-coupled nanocomputing,” *Journal of Low Power Electronics and Applications*, vol. 12, no. 1, 2022.